Catalysts **2011**, *1*, 3-17; doi:10.3390/catal1010003

OPEN ACCESS

catalysts

ISSN 2073-4344

www.mdpi.com/journal/catalysts

Review

Atomically Monodisperse Gold Nanoclusters Catalysts with Precise Core-Shell Structure

Yan Zhu [1,2,*], Rongchao Jin [2] and Yuhan Sun [1,*]

[1] Low Carbon Conversion Center, Shanghai Advanced Research Institute, Chinese Academy Sciences, Shanghai 201203, China

[2] Department of Chemistry, Carnegie Mellon University, Pittsburgh, PA 15213, USA; E-Mail: rongchao@andrew.cmu.edu

* Author to whom correspondence should be addressed; E-Mails: zhuyan@andrew.cmu.edu (Y.Z.); sunyh@sari.ac.cn (Y.S.).

Received: 26 July 2011; in revised form: 26 August 2011 / Accepted: 29 August 2011 / Published: 7 September 2011

Abstract: The emphasis of this review is atomically monodisperse Au_n nanoclusters catalysts (n = number of metal atom in cluster) that are ideally composed of an exact number of metal atoms. Au_n which range in size from a dozen to a few hundred atoms are particularly promising for nanocatalysis due to their unique core-shell structure and non-metallic electronic properties. Au_n nanoclusters catalysts have been demonstrated to exhibit excellent catalytic activity in hydrogenation and oxidation processes. Such unique properties of Au_n significantly promote molecule activation by enhancing adsorption energy of reactant molecules on catalyst surface. The structural determination of Au_n nanoclusters allows for a precise correlation of particle structure with catalytic properties and also permits the identification of catalytically active sites on the gold particle at an atomic level. By learning these fundamental principles, one would ultimately be able to design new types of highly active and highly selective gold nanocluster catalysts for a variety of catalytic processes.

Keywords: Au_n nanoclusters; core-shell; atomically monodisperse; structure-catalysis

---

1. Introduction

Gold was initially considered to be catalytically inactive for a long time [1,2]. This changed when gold was seen in the context of the nanometric scale, which has indeed shown it to have excellent catalytic activity as a homogeneous or a heterogeneous catalyst [3-12]. The comprehensive reviews and books about gold nanoparticles as catalysts have appeared, which cover many important aspects related to preparation of gold catalysts and their catalytic properties [13-19]. However, almost all of the current studies only give rise to an ensemble average of the catalytic performance due to the structural polydispersity and heterogeneity of conventional nanoparticles catalysts. Although significant efforts have been invested in preparing well defined nanoparticles, fundamental nanocatalysis research still lags significantly behind. Due to the size dispersity of conventional nanoparticles, it is not possible to achieve an in-depth understanding of the origin of the size-dependence of nanogold catalysts; moreover, it is impossible to identify the catalytically active species in nanoparticle catalysis.

Therefore, it is of paramount importance to attain atomically precise gold nanoparticles and use such nanoparticles as well defined catalysts. By solving their atomic structure of the nanoparticles, one will be able to precisely correlate the catalytic properties with the exact atomic structure of the nanoparticles and to learn what controls the surface activation, surface active site structure and catalytic mechanism. Atomically monodisperse gold nanoclusters (referred to as Au_n, n = number of metal atom in particle, n ranging from a dozen to hundreds) are ideally composed of an exact number of gold atoms and are unique and vastly different from their larger counterparts—gold nanocrystals (typically 3–100 nm). Small Au_n nanoclusters ($n < 100$) behave like molecules and exhibit strong quantum confinement effects; relatively larger ones ($100 < n < 200$) exhibit intermediate properties between molecular behavior and metallic properties [20]. Overall, the non-metallic behavior of Au_n in both size regimes is particularly important for nanocatalysis. More importantly, on the basis of their atom packing structures and unique electronic properties, one could indeed study a precise correlation of structural properties with catalytic properties, identify the catalytically active sites on the gold particle and unravel the nature of gold catalysis [21-27]. This has long been an important task in nanocatalysis [28-36].

The emphasis of the review will be on the preparation of monodisperse gold nanocluster catalysts and precise structure-catalytic activity relationships, the investigation of which is currently being actively pursued.

2. Atomic Structure of Gold Nanoclusters

The atom packing structures of Au_n nanoclusters are critical for understanding the catalytic properties of nanoclusters and theoretical modeling of mechanistic steps. The synthesis of gold nanoclusters in solution phase has been developed, including the electrophoretic separation [37,38], the kinetic control approach [39,40], and the thiol etching method [41,42]. Interestingly, these structures of Au_n nanoclusters do not resemble the face-centered cubic (fcc) structure of their larger counterparts: gold nanocrystals or bulk gold. Firstly, the structural model emerged from the density functional calculation provides a glimpse into a prevailing structural concept with an atomically Au/ligand interface and compact gold core [43-57].

The early theoretical studies confirmed that Au_{16} and Au_{20} clusters have tetrahedral structures. Au_{20} cluster contains a prolate Au_8 core and four level-3 extended staple motifs -RS-Au-RS-Au-RS-Au-RS-. This highly stable cluster may represent a structural evolution of thiolate protected gold clusters from the homoleptic core-free structure to the core-stacked structure (Figure 1) [58]. The geometry of Au_{16} is derived from the T_d-symmetric Au_{20} by removing the four vertex atoms and allowing for an outward relaxation of the 4 face-centered atoms [59]. Au_{34} cluster has been predicted for a C_3 structure constructured from a more symmetric C_{3v} geometry via a twist (see Figure 2) [60]. Au_{39} cluster has an approximate D_3 point group symmetry, with the gold atoms forming a hexagonal antiprismatic cage, filled by one bulk-coordinated gold atom (Figure 3) [61].

Figure 1. Structures of Au_{20} cluster and structural decomposition of the Au_8 core and four level-3 staple motifs [58].

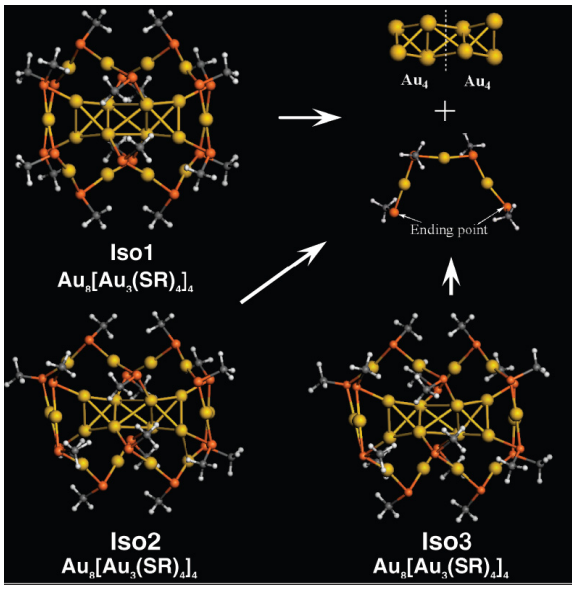

Figure 2. Two views of Au_{34} cluster with C_{3v} symmetry and C_3 symmetry [60].

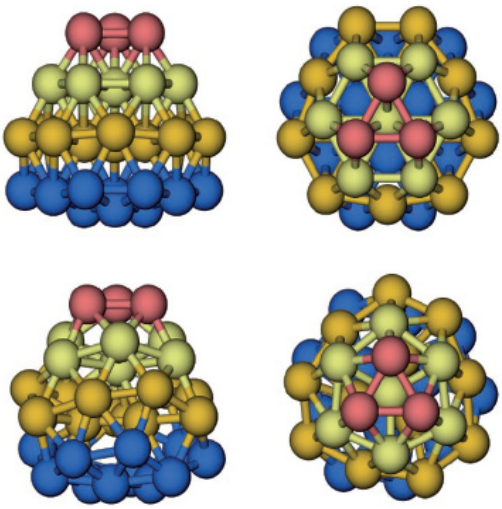

Figure 3. (**A**) The structure of Au_{39} cluster; and (**B**) Au core of Au_{39} [61].

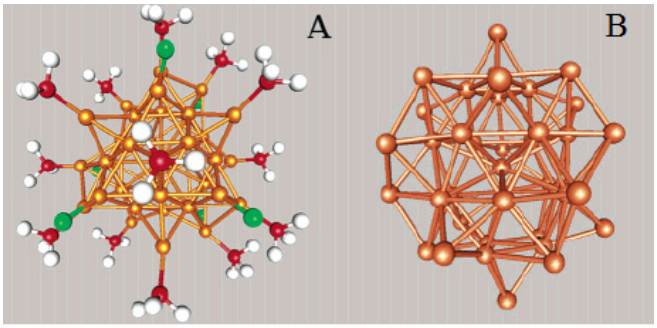

The true monodispersity of Au_n nanoclusters allows us to grow single crystals and determines their total structures by X-ray crystallography [62-65]. By carefully controlling the experimental conditions of the nanocluster synthesis, a specific chemical environment is created, which leads to exclusive formation of atomically precise, one-sized Au_n nanoclusters in high yield and high purity. The experimental breakthroughs focus on the crystal structures of three $Au_n(SR)_m$ nanoclusters, including $Au_{102}(S\text{-}C_6H_4\text{-}p\text{-}COOH)_{44}$, $Au_{25}(SC_2H_4Ph)_{18}$, and $Au_{38}(SC_2H_4Ph)_{24}$. We start with the smallest $Au_{25}(SR)_{18}$ cluster. The control kinetics toward the synthesis of one-sized Au_{25} cluster involves two steps (Figure 4): (i) the reduction of Au(III) to Au(I) by thiols, forming an intermediate of Au-(I):SR complexes; and (ii) further reduction of Au(I) to Au(0) by a strong reducing agent ($NaBH_4$). The control over the reaction temperature (0 °C) and stirring condition can generate a particular aggregation state of the Au(I):SR intermediates that leads to the exclusive formation of Au_{25} nanoclusters [39].

Figure 4. The preparation of Au_{25} nanoclusters [39].

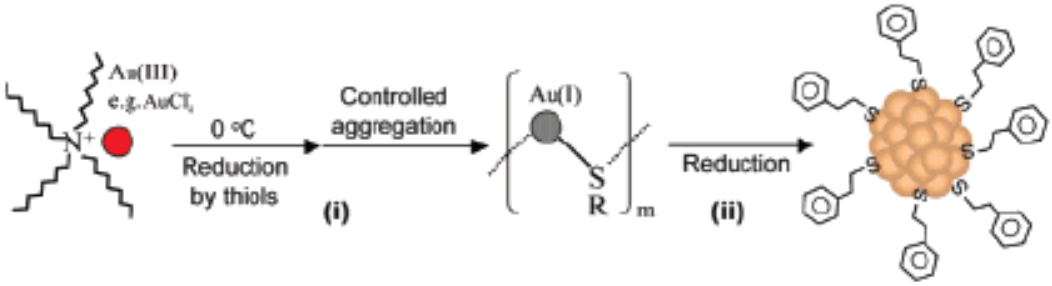

X-ray crystallographic analysis shows that the Au_{25} nanocluster features a centered icosahedral Au_{13} core (Figure 5(A)), further capped by a second shell comprised of the remaining 12 Au atoms [64]. Viewed along the three mutually perpendicular C_2 axes of the icosahedron, the 12 exterior Au atoms form six pairs and are situated around the ±x, ±y, and ±z axes, respectively (Figure 5(B)). Another view of the $Au_{25}(SR)_{18}$ structure is an Au_{13} icosahedral kernel capped by six staple motifs of –S(R)–Au–S(R)–Au–S(R)– along the ±x, ±y, and ±z axes (Figure 5(C)). Apparently, the 12 exterior Au atoms form an open shell on the Au_{13} icosahedron. An icosahedron has 20 triangular faces (Au_3), but only 12 of them are face-capped, which leaves eight Au_3 triangular faces uncapped. The entire Au_{25} cluster is protected by 18 –SR ligands. The charge state (q = −1, 0) of $[Au_{25}(SR)_{18}]^q$ does not affect the atomic structure of the cluster [66,67].

Figure 5. Anatomy of the atom packing structure of $Au_{25}(SR)_{18}$ nanocluster [64].

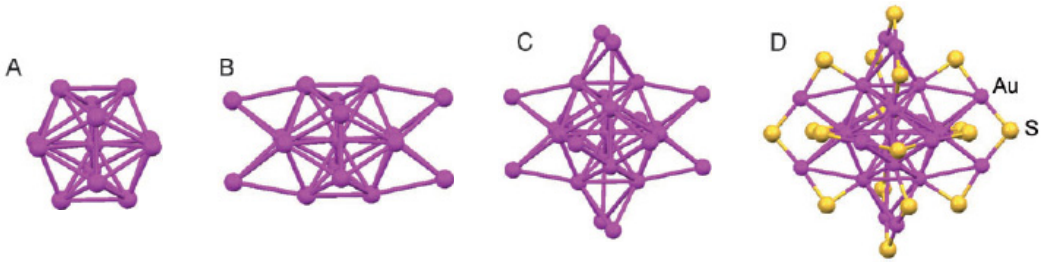

The next size is the 38-atom $Au_{38}(SR)_{24}$ [65,68]. The high yield synthesis of monodisperse Au_{38} nanoclusters involves two main steps (Figure 6): first, glutathionate (-SG) protected polydisperse Au_n clusters (n ranging from 38 to 102) are synthesized by reducing Au(I)-SG in acetone; subsequently, the size-mixed Au_n clusters react with excess phenylethylthiol (PhC_2H_4SH) for 40 h at 80 °C, which leads to $Au_{38}(SC_2H_4Ph)_{24}$ clusters of molecular purity.

Figure 6. A two-step procedure for synthesizing monodisperse $Au_{38}(SC_2H_4Ph)_{24}$ clusters in high yield [68].

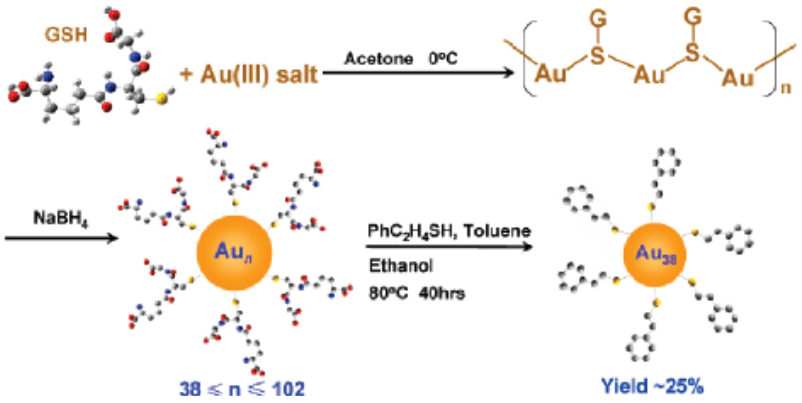

The core of $Au_{38}(SR)_{24}$ is a face-fused biicosahedral Au_{23} (13 + 13 − 3 = 23) (Figure 7(A)) [65]. The fusion of the two icosahedra occurs along a common C_3 axis. Note that the way the structure is anatomized does not necessarily mean the real growth mechanism of the cluster. The Au_{23} rod is structurally strengthened by three monomeric -SR-Au-RS- staples (Figure 7(C)). Then, the top icosa-hedron is further capped by three -SR-Au-SR-Au-RS- dimeric staples, which are arranged in a rotative fashion, resembling a tri-blade "fan" or "propeller" (Figure 7(D) and (E)). A similar arrangement of the other three staples is found on the bottom icosahedron, but the bottom "propeller" rotates by approximately 60° relative to the top one, forming a staggered dual-propeller configuration. In fact, the entire cluster is chiral due to the rotative arrangement of the dimeric staples. A larger $Au_n(SR)_m$ nanocluster is $Au_{102}(SR)_{44}$ [62,69]. The gold particles were coated with p-MBA and crystallized from a solution containing 40% methanol, 300 mM sodium chloride, and 100 mM sodium acetate, at pH 2.5. Interestingly, this cluster has a truncated Au_{49} Marks decahedral kernel (Figure 8B and C), which is based on a fivefold symmetric 19-atom kernel (Figure 8(A)). The Au_{49} kernel is further capped by two 15-atom caps at the top/bottom, respectively (Figure 8(D) and (E)). The resultant Au_{79} kernel is capped by five -SR-Au-SR- monomeric staples on the top and another five at the bottom, and nine monomers

and two dimers (-SR-Au-SR-Au-SR-) at the waist. The arrangement of 13 gold atoms at the waist (from nine monomers and two dimers, $9 + 2 \times 2 = 13$) destroys the fivefold symmetry of the entire Au_{102} cluster, so Au_{102} cluster has two chiral isomers.

Figure 7. Anatomy of the atom packing structure of $Au_{38}(SR)_{24}$ nanocluster [65].

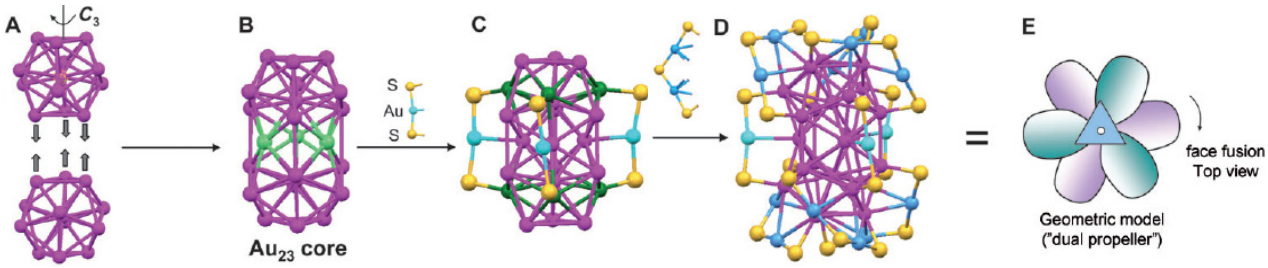

Figure 8. Anatory of $Au_{102}(SR)_{44}$ structure: (**A**) fivefold symmetric 19-atom (Au_{19}) kernel; (**B**,**C**) side and top views of Au_{49} Marks decahedron; (**D**,**E**) side and top views of Au_{79} kernel; (**F**) overall framework of $Au_{102}S_{44}$ (R groups are omitted for clarity) [69].

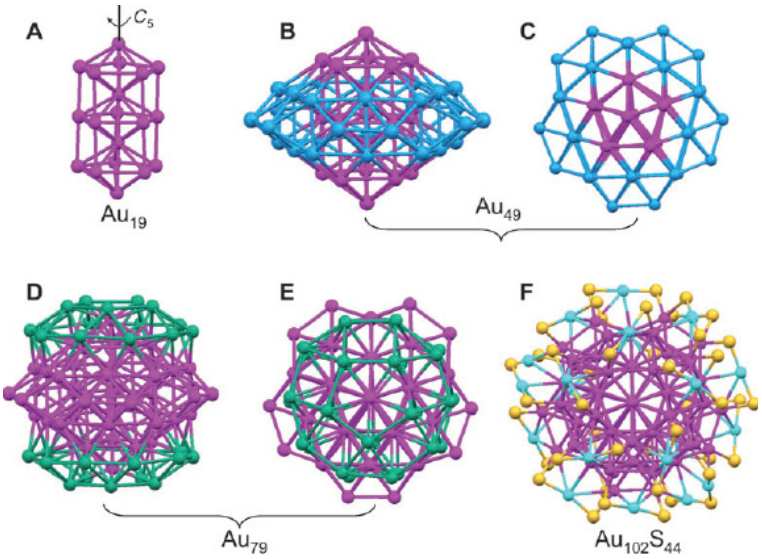

3. Catalytic Performance of Atomically Precise Gold Nanocluters

Such nanoclusters provide a new opportunity for unraveling catalysis at an atomic level. The catalytic activity has been explained by various complementary mechanisms, such as charging effects, geometric fluxionality, particle-size-dependent metal-insulator transition and electronic quantum size effects [70-76]. The theoretical investigations of the catalytic activity of these small gold nanoclusters (up to a few tens of atoms) were studied a decade ago [29,75]. Density functional calculations showed that the gold particle sizes fall into a region where quantum size effects are expected to dominate the reactivity of gold. Hakkinen *et al*. showed, by considering a series of structurally well-defined gold clusters with diameter between 1.2 and 2.4 nm, that electronic quantum size effects, particularly the magnitude of HOMO-LUMO energy gap, have a decisive role in activated-form of the nanocatalysts [70].

Figure 9. Atomic structure for the most favorable energy profile for O_2 dissociation on Au_{38} cluster [75].

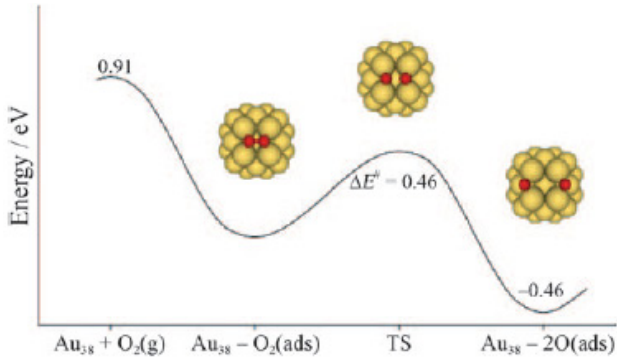

The experiments have given strong indications of the catalytic activity of supersmall well-defined gold clusters. Recently, Turner *et al.* [77] reported the selective oxidation of styrene with O_2 by nanocatalysts derived from solution phase protected Au_{55} clusters and found the activity of Au_{55} nanocatalyst was super to that of Au nanocrystals (>3 nm). A sharp size threshold in catalytic activity was found such that that, when fed with O_2 alone, the catalytic activity is quenched for Au particles with diameters greater than or equal to 2 nm (Figure 10(d)). Since the crystal structure of Au_{55} cluster has been utterly unknown so far, it is not easy to correlate structural properties with catalytic properties.

Figure 10. TEM images of overlaid with corresponding particle size distribution for Au_{55} nanocluster [77].

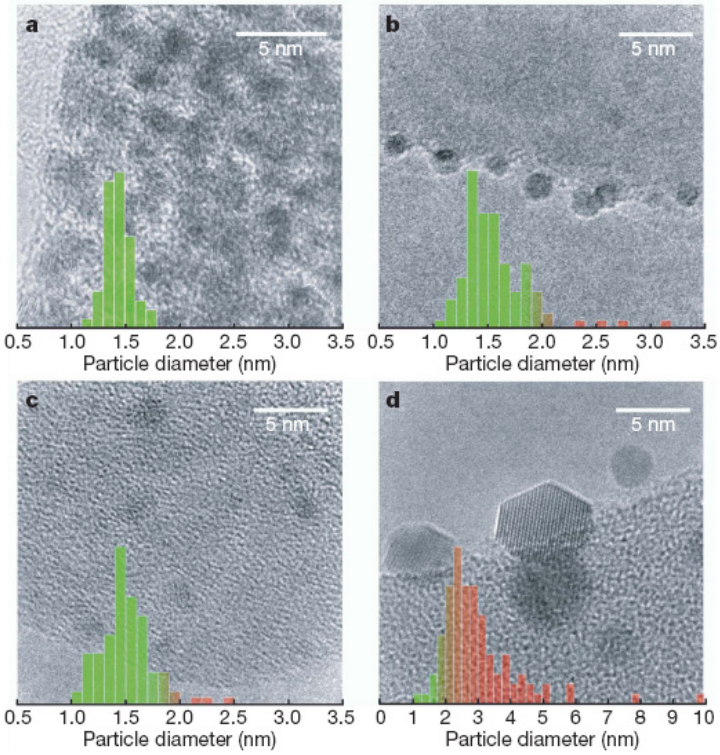

Tsukuda *et al.* studied the effect of electronic structures of Au clusters on aerotic oxidation catalysis [78-80]. The catalytic activity is enhanced with increasing electron density on the Au core.

They proposed that electron transfer from the anionic gold core into LUMO(π*) of O_2 forms superoxo- or peroxo-like species, which may play an essential role in the oxidation of alcohol (Figure 11). This work provides a principle for the synthesis of aerobic oxidation catalysts based on the electronic structures of Au clusters and more electronic charge should be deposited into the high-lying orbitals of Au clusters by doping with electropositive elements or by interaction with nucleophilic sites of stabilizing molecules.

Figure 11. Mechanism for the activation of molecular oxygen by Au cluster [78].

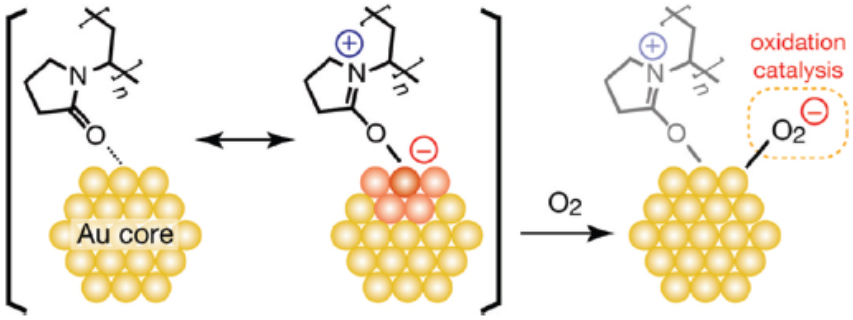

Recently, Jin *et al.* reported the $Au_n(SR)_m$ nanocluster catalysts for selective oxidation of styrene using three robust supersmall Au_n nanoclusters, including Au_{25} (1.0 nm), Au_{38} (1.3 nm) and Au_{144} (1.6 nm) [23,26]. The catalytic activity of Au_n nanocluster catalysts exhibits a strong dependence on size (*n*); the smaller $Au_n(SR)_m$ nanoclusters give rise to a much higher catalytic activity. Among the three sizes, Au_{25} nanocluster catalyst shows the highest conversion of styrene, followed by Au_{38} and Au_{144}. The effect of thiolate ligands was investigated and found that the ligands do not affect the catalytic activity and selectivity. Therefore, the catalysis of Aun(SR)m nanoclusters are mainly determined by the gold core rather than by ligands shell. A mechanism has been proposed for selective oxidation of styrene catalyzed by $Au_{25}(SR)_{18}$ nanoclusters (Figure 12) [26]. The three oxidant systems were investigated: (a) TBHP (*tert*-butyl hydroperoxide) as the oxidant; (b) TBHP as an initiator and O_2 as the main oxidant; (c) O_2 as the oxidant [26]. The three different oxidant systems can undergo different reaction pathways to activate the oxidants and generate a common peroxyformate intermediate Au_{25}-$O_{2(ad)}$ (species D). In the case of TBHP as the oxidant, interaction of anionic Au_{25} (species A) with TBHP forms a hydroperoxy species B, and then species B loses one H_2O molecule and rearranges to form the Au_{25}-$O_{2(ad)}$ species D. In the case of TBHP as an initiator and O_2 as a main oxidant, initiation of TBHP forms species BuO*/*OH and hence activates O_2 to form the superoxo-like O_2*. The O_2* is proposed to adsorb *via* a side-on fashion to the gold surface with two partial Au-O bonds to produce a low-barrier transition state species C, and then the peroxo-like species C transforms to the Au_{25}-$O_{2(ad)}$ species D. In the case of sole O_2 as oxidant, O_2 may directly attack the Au_{13} core to form the Au_{25}-$O_{2(ad)}$ species D. The presence of partial positive charges on the surface gold atoms of the Au_{12} shell should greatly facilitate activation of the nucleophilic C=C group of styrene (species E) since the positive Au atoms at the shell are electrophilic. Then the activated C=C bond reacts with the $O_{2(ad)}$ species through side-by-side interaction on the Au_{25} surface sites, leading to species F. Subsequently, the catalytic selectivity is triggered by the dissociation and rearrangement in three competing pathways that lead to the three products. The formation of benzaldehyde is from the

breaking of the C–C bond (species G); the epoxide is created by the transfer of oxygen to the olefinic bond to form a metalloepoxy intermediate (species H); and acetophenone is produced by the breaking of the C–O bond (species I). Finally, the oxidized $[Au_{25}(SR)_{18}]^0$ catalyst can be reduced to the anionic $[Au_{25}(SR)_{18}]^-$ by gaining an electron when the C=C bond leaves the Au_{25} cluster, hence, one catalytic cycle is completed [26].

Figure 12. The proposed mechanism of selective oxidation of styrene catalyzed by $[Au_{25}(SR)_{18}]_q$ clusters [26].

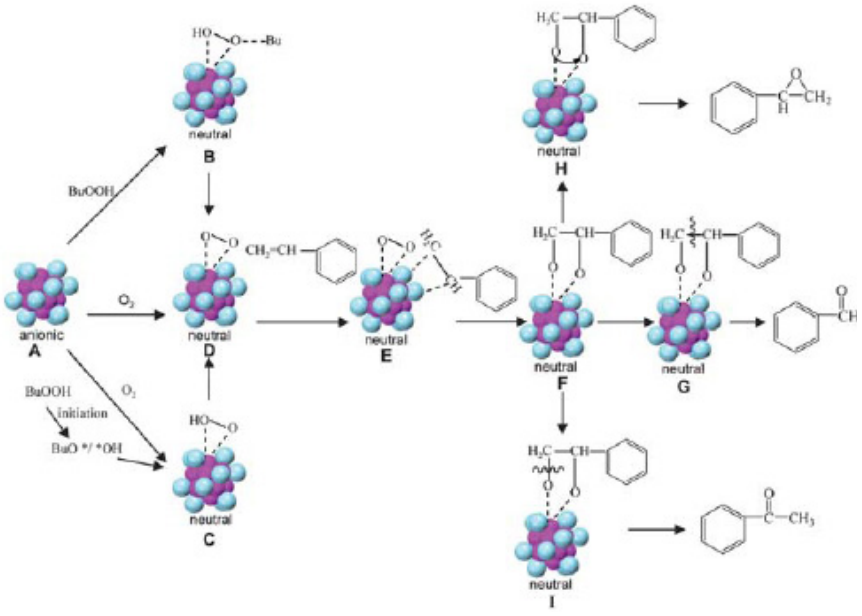

Tsukuda *et al.* [22] immobilized $Au_{25}(SR)_{18}$ nanoclusters on a hydroxyapatite support for the selective oxidation of styrene in toluene solvent. They achieved a 100% conversion of styrene and 92% selectivity to the epoxide product. These results demonstrate that atomically monodisperse Au_n nanocluster catalysts exhibit excellent catalytic activity in the selective oxidation processes.

Au_n nanolcusters catalysts have also made significant advances in selective hydrogenation processes. Herein, Au_{25} nanocluster is chosen as a model for a discussion of selective hydrogenation. The crystal structures of $[Au_{25}(SR)_{18}]^q$ ($q = -1, 0$) show a core–shell type structure: a Au_{13} icosahedral core and an exterior Au_{12} shell. The charge distribution on the Au_{13} core and the Au_{12} shell is quite different: the Au_{13} core possesses eight (when $q = -1$) or seven (q = 0) delocalized valence electrons originated from Au(6s). These electrons are primarily distributed within the Au_{13} core, whereas the Au_{12} shell bears positive charges due to bonding with thiolates and electron transfer from gold to sulfur. The electron-rich Au_{13} core should facilitate electrophilic bands activation, such as C=O, accompanied by conversion of $[Au_{25}(SR)_{18}]^-$ to neutral $[Au_{25}(SR)_{18}]^0$. An Au_{12} shell with low-coordination charater should adsorpt and dissociate H_2.

Selective hydrogenation of α,β-unsaturated ketones/aldehydes, conventional supported gold nanoparticle catalysts have been demonstrated to be capable of selective hydrogenation of α,β-unsaturated ketones to produce predominant α,β-unsaturated alcohols but with side products of saturated ketones from C=C hydrogenation as well as saturated alcohols from further hydrogenation. Although conventional gold nanoparticles can achieve high conversion and selectivity of the

unsaturated alcohol in the hydrogenation of α,β-unsaturated ketones, a ~100% selectivity for the unsaturated alcohol has not been achieved [21]. Using $Au_{25}(SR)_{18}$ nanoclusters as hydrogenation catalysts, selective hydrogenation of the C=O bond in α,β-unsaturated ketones (or aldehydes) with 100% selectivity for α,β-unsaturated alcohols can be obtained. The extraordinary selectivity and activity of Au_{25} catalysts correlate with the electronic structure of the Au_{25} nanocluster and its non-closed Au_{12} exterior shell. The volcano-like eight uncapped Au_3 faces of the icosahedron from the exposure of Au_{13} core should favor adsorption of the C=O group by interaction of the active site with the O atom of the C=O group (see Figure 13). Subsequently, the weakly nucleophilic hydrogen attacks the activated C=O group, and then form the unsaturated alcohol product. The surface Au atoms with low-coordination character, coordination number N = 3, should provide a favorable environment for the adsorption and dissociation of H_2, and H_2 dissociation should occur on the gold atoms of the exterior shell (Figure 13) [21]. The electron-rich Au_{13} core has no ability to active C=C bond in α,β-unsaturated ketone at mild temperatures, therefore there are no side products from the hydrogenation of C=C in α,β-unsaturated ketone.

Figure 13 . Proposed mechanism of $Au_{25}(SR)_{18}$ nanocatalysis for the chemoselective hydrogenation of α,β-unsaturated ketone to unsaturated alcohol (pink: Au atoms of the core, blue: Au atoms of the shell [21].

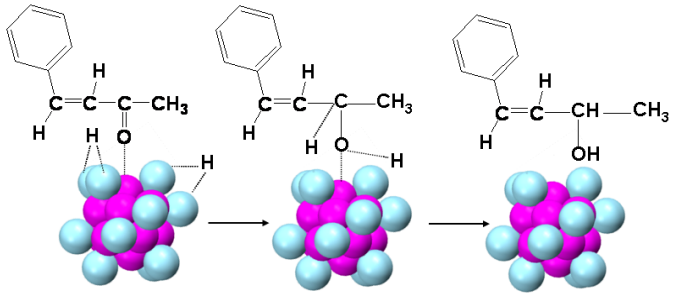

4. Conclusions

These Au_n catalyst examples demonstrate the huge power of atomically precise Au_n nanocatalysts for achieving super selective oxidation and hydrogenation performance and atomically precise structure-property relationships. Au_n nanoclusters possess a unique core-shell structure—an electron-rich core with delocalized valence electrons and an electron-deficient shell. Such nanoclusters will not only provide further insight into the nature of gold nanocatalysis at an atomic level, but also promote the exploration of new chemical processes with Au_n as well-defined, highly efficient catalysts. Au_n nanocluster catalysts will ultimately bring gold nanocatalysis to an exciting new level.

References

1. Armer, B.; Schmidbaur, H. Organogoldchemie. *Angew. Chem.* **1970**, *82*, 120-133.
2. Bond, G.C. The catalytic properties of gold. *Gold Bull.* **1972**, *5*, 11-13.
3. Bond, G.C.; Sermon, P.A.; Webb, G.; Buchanan, D.A.; Well, P.B. Hydrogenation over supported gold catalysts. *J. Chem. Soc. Chem. Commun.* **1973**, 444-445.

4. Hutchings, G.J. Vapor phase hydrochlorination of acetylene: Correction of catalysis activity of supported metal chloride catalysts. *J. Catal.* **1985**, *96*, 292-295.
5. Hayashi, T.; Tanaka, K.; Haruta, M. Selective vapor-phase epoxidation of propylene over Au/TiO2 catalysts in the presence of oxygen and hydrogen. *J. Catal.* **1998**, *178*, 566-575.
6. Hashmi, A.S.K.; Schwarz, L.; Choi, J.H.; Frost, T.M. Eine neue Gold-katalysierte C–C Bindungknupfung. *Angew. Chem.* **2000**, *112*, 2382-2385.
7. Guzman, J.; Gates, B.C. Catalysis by supported gold: Correlation between catalytic activity for CO oxidation and oxidation states of gold. *J. Am. Chem. Soc.* **2004**, *126*, 2672-2673.
8. Min, B.K.; Friend, C.M. Heterogeneous gold-based catalysis for green chemistry: Low-temperature CO oxidation and propene oxidation. *Chem. Rev.* **2007**, *107*, 2709-2724.
9. Della, P.C.; Falletta, E.; Prati, L.; Rossi, M. Selective oxidation using gold. *Chem. Soc. Rev.* **2008**, *37*, 2077-2095.
10. Chen, M.S.; Kumar, D.; Yi, C.W.; Goodman, D.W. The promotional effect of gold in catalysis by palladium-gold. *Science* **2005**, *310*, 291-293.
11. Grirrane, A.; Corma, A.; Garcia, H. Gold-catalyzed synthesis of aromatic azo compounds from anilines and nitroaromatics. *Science* **2008**, *322*, 1661-1664.
12. Fang, W.H.; Chen, J.S.; Zhang, Q.H.; Deng, W.P.; Wang, Y. Hydrotalcite-supported gold catalyst for the oxidant-free dehydrogenation of benzyl alcohol: Studies on support and gold size effect. *Chem. Eur. J.* **2011**, *17*, 1247-1256.
13. Bond, G.C.; Louis, C.; Thompson, D.T.; Hutchings, G.J. *Catalysis by Gold*; Imperial College: London, UK, 2006.
14. Heiz, U.; Landman, U. *Nanocatalysis*; Spring: New York, NY, USA, 2007.
15. Hashmi, A.S.K.; Hutching, G.J. Gold catalysis. *Angew. Chem. Int. Ed.* **2006**, *45*, 7896-7936.
16. Jimenez-Nunez, E.; Echavarren, A.M. Molecular diversity through gold catalysis with alkynes. *Chem. Commun.* **2007**, 333-346.
17. Corma, A.; Garcia, H. Supported gold nanoparticles as catalysts for organic reactions. *Chem. Soc. Rev.* **2008**, *37*, 2096-2126.
18. Daniel, M.C.; Didier, A. Gold nanoparticles: Assembly, supramolecular chemistry, quantum-size-related properties, and applications toward biology, catalysis and nanotechnology. *Chem. Rev.* **2004**, *104*, 293-346.
19. Ma, Z.; Dai, S. Design of novel structured gold nanocatalysts. *ACS Catal.* **2011**, *1*, 805-818.
20. Jin, R.C.; Qian, H.F.; Zhu, Y.; Das, A. Atomically precise nanoparticles: A new frontier in nanoscience. *J. Nanosci. Lett.* **2010**, *1*, 72-86.
21. Zhu, Y.; Qian, H.F.; Drake, B.A.; Jin, R.C. Atomically precise $Au_{25}(SR)_{18}$ nanoparticles as catalysts for selective hydrogenation of α,β-unsaturated ketones and aldehydes. *Angew. Chem. Int. Ed.* **2010**, *49*, 1295-1298.
22. Liu, Y.; Tsunoyama, H.; Akita, T.; Tsukuda, T. Efficient and selective epoxidation of styrene with TBHP catalyzed by Au25 clusters on hydroxyapatite. *Chem. Commun.* **2010**, *46*, 550-552.
23. Zhu, Y.; Qian, H.F.; Zhu, M.Z.; Jin, R.C. Thiolate-protected Au_n nanoclusters as catalysts for selective oxidation and hydrogenation processes. *Adv. Mater.* **2010**, *22*, 1915-1920.
24. Zhu, Y.; Wu, Z.K.; Gayathri, C.; Qian, H.F.; Gil, R.R.; Jin, R.C. Exploring stereoselectivity of Au_{25} nanoparticle catalyst for hydrogenation of cyclic ketone. *J. Catal.* **2010**, *271*, 155-160.

25. Qian, H.F.; Barry, E.; Zhu, Y.; Jin, R.C. Doping 25-atom and 38-atom gold nanoclusters with palladium. *Acta Phys. Chim. Sin.* **2011**, *27*, 513-519.
26. Zhu, Y.; Qian, H.F.; Jin, R.C. An atomic-level strategy for unraveling gold nanocatalysis from the perspective of $Au_n(SR)_m$ nanoclusters. *Chem. Eur. J.* **2010**, *16*, 11455-11462.
27. Zhu, Y.; Qian, H.F.; Jin, R.C. A comparison of the catalytic properties of atomically precise, 25-atom gold nanospheres and nanorods. *Chin. J. Catal.* **2011**, *32*, 1145-1150.
28. Somaijai, G.A. *Introduction to Surface Chemistry and Catalysis*; Wiley: New York, NY, USA, 1994.
29. Sanchez, A.; Abbet, S.; Heiz, U.; Schneider, W.D.; Hakkinen, H.; Barnett, R.N.; Landman, U. When gold is not noble: Nanoscale gold catalysts. *J. Phys. Chem. A* **1999**, *103*, 9573-9578.
30. Haruta, M.; Date, M. Advances in the catalysis of Au nanoparticles. *Appl. Catal. A* **2001**, *222*, 427-437.
31. Meyer, R.; Lemire, C.; Shaikhutdinov, Sh.K.; Freund, H.J. Surface chemistry of catalysis by gold. *Gold. Bull.* **2004**, *37*, 72-124.
32. Maye, M.M.; Luo, J.; Han, J.; Kariuki, N.N.; Zhong, C.J. Synthesis, processing, assembly and activation of core-shell structural gold nanoparticle catalysts. *Gold. Bull.* **2003**, *36*, 75-82.
33. Herzing, A.A.; Kiely, C.J.; Carley, A.F.; Lond, P.; Hutchings, G.J. Identification of active gold nanoclusters on iron oxide supports for CO oxidation. *Science* **2008**, *321*, 1331-1335.
34. Murakami, Y.; Konishi, K. Remarkable co-catalyst effect of gold nanoclusters on olefin oxidation catalyzed by a manganese-porphyrin complex. *J. Am. Chem. Soc.* **2007**, *129*, 14401-14407.
35. Fierro-Gonzalez, J.C.; Gates, B.C. Catalysis by gold dispersed on supports: The importance of cationic gold. *Chem. Soc. Rev.* **2008**, *37*, 2127-2134.
36. Grabow, L.C.; Mavrikakis, M. Nanocatalysis beyond the gold-rush era. *Angew. Chem. Int. Ed.* **2008**, *47*, 7390-7392.
37. Negishi, Y.; Nobusada, K.; Tsukuda, T. Glutathione-protected gold revisited: Bridging the gap between gold(I)-thiolate complexed and thiolate-protected gold nanocrystals. *J. Am. Chem. Soc.* **2005**, *127*, 5261-5270.
38. Schaaff, T.G.; Knight, G.; Shafigullin, M.N.; Borkman, R.F.; Whetten, R.L. Isolation and selected properties of a 10.4 kDa gold: Glutathione cluster compound. *J. Phys. Chem. B* **1998**, *102*, 10643-10636.
39. Zhu, M.; Lanni, E.; Garg, N.; Bier, M.E.; Jin, R.C. Kinetically controlled, high-yield synthesis of Au_{25} cluster. *J. Am. Chem. Soc.* **2008**, *130*, 1138-1139.
40. Wu, Z.K.; MacDonald, M.A.; Chen, J.; Zhang, P.; Jin, R.C. Kinetic control and thermodynamic selection in the synthesis of atomically precise gold nanoclusters. *J. Am. Chem. Soc.* **2011**, *133*, 9670-9673.
41. Tchaaff, T.G.; Whetten, R.L. Controlled etching of Au:SR clusters compounds. *J. Phys. Chem. B* **1999**, *103*, 9394-9396.
42. Chaki, K.; Negishi, Y.; Tsunoyama, H.; Shichibu, Y.; Tsukuda, T. Ubiquitous 8 and 29 kDa gold:alkanethiolate cluster compounds: Mass-spectrometric determination of molecular formulas and structuralimplications. *J. Am. Chem. Soc.* **2008**, *130*, 8608-8610.
43. Hakkinen, H. Atomic and electronic structure of gold clusters: Understanding flakes, cages and superatoms from simple concerpts. *Chem. Soc. Rev.* **2008**, *37*, 1847-1859.

44. Gilb, S.; Weis, P.; Furche, F.; Ahlrichs, R.; Kappes, M.M. Structure of small gold cluster cations (Au^{+}_{n}, n < 14): Ion mobility measurements versus density functional calculations. *J. Chem. Phys.* **2002**, *116*, 4094-4101.
45. Li, J.; Li, X.; Zhai, H.J.; Wang, L.S. Au20: A tetrahedral cluster. *Science* **2003**, *299*, 864-867.
46. Yoon, B.; Koskinen, P.; Huber, B.; Kostko, O.; Issendorff, B.V.; Hakkinen, H.; Moseler, M.; Landman, U. Size-dependent structural evolution and chemical reactivity of gold clusters. *Chem. Phys. Chem.* **2007**, *8*, 157-161.
47. Kondo, Y.; Takayanagi, K. Synthesis and characterization of helical multi-shell gold nanowires. *Science* **2000**, *289*, 606-608.
48. Price, R.; Whetten, R.L. Structure of a thiol monolayer-protected gold nanoparticle at 1.1 Å resolution. *Science* **2007**, *318*, 407-408.
49. Akola, J.; Walter, M.; Whetten, R.L.; Hakkinen, H.; Gronbeck, H. On the structure of thiolate-protected Au_{25}. *J. Am. Chem. Soc.* **2008**, *130*, 3756-3757.
50. Walter, M.; Akola, J.; Lopez-Acevedo, O.; Jadzinsky, P.D.; Calero, G.; Ackerson, C.J.; Whetten, R.L.; Gronberk, H.; Hakkinen, H. A unified view of liang-protected gold clusters as superatom complexs. *Proc. Natl. Acad. Sci. USA* **2008**, *105*, 9157-9162.
51. Jiang, D.E.; Chen, W.; Whetten, R.L.; Chen, Z.F. What protect the core when the thiolated Au cluster is extremely small. *J. Phys. Chem. C* **2009**, *113*, 16983-16987.
52. Lopez-Acevedo, O.; Akola, J.; Whetten, R.L.; Gronbech, H.; Hakkinen, H. Structure and bonding in the ubiquitous icosuhedral metallic gold cluster $Au_{144}(SR)_{60}$. *J. Phys. Chem. C* **2009**, *113*, 5035-5038.
53. Schrid, G. The relevance of shape and size of Au_{55} clusters. *Chem. Soc. Rev.* **2008**, *37*, 1909-1930.
54. Jin, R.C. Quantum sized, thiolate-protected gold nanoclusters. *Nanoscale* **2010**, *2*, 343-362.
55. Shichibu, Y.; Negishi, Y.; Watanabe, T.; Chaki, N.K.; Kawaguchi, H.; Tsukuda, T. Biicosahedral gold clusters $[Au_{25}(PPh_3)_{10}(SC_nH_{2n+1})_5Cl_2]^{2+}$ (n = 2–18): A stepping stone to cluster-assembled materials. *J. Phys. Chem. C* **2007**, *111*, 7845-7847.
56. Wen, F.; Englert, U.; Gutrath, B.; Simon, U. Crystal structure, electrochemical and optical properties of $[Au_9(PPh_3)_8](NO_3)_3$. *Eur. J. Inorg. Chem.* **2008**, 106-111.
57. Johansson, M.P.; Sundholm, D.; Vaara, J. Au32: A 24-carat golden fullerene. *Angew. Chem. Int. Ed.* **2004**, *43*, 2678-2681.
58. Pei, Y.; Gao, Y.; Shao, N.; Zeng, X.C. Thiolate-pretected $Au_{20}(SR)_{16}$ cluster: Prolate Au_8 core with new $[Au_3(SR)_4]$ staple motif. *J. Am. Chem. Soc.* **2009**, *131*, 13619-13621.
59. Walter, M.; Hakkinen, H. A hollow tetrahedral cage of hexadecagold dianion provides a robust backbone for a tuneable sub-nanometer oxidation and reduction agent *via* endohedral doping. *Phys. Chem. Chem. Phys.* **2006**, *8*, 5407-5411.
60. Lechtken, A.; Schooss, D.; Stairs, J.R.; Blom, M.N.; Furche, F.; Morgner, N.; Kostko, B.; Kappes, M.M. Au_{34}^{-}: A chrial gold cluster. *Angew. Chem. Int. Ed.* **2007**, *46*, 2944-2948.
61. Hakkinen, H.; Walter, M.; Gronbeck, H. Divide and protect: Capping gold nanoclusters with molecular gold-thiolate rings. *J. Phys. Chem. B* **2006**, *110*, 9927-9931.

62. Pablo D.; Jadzinsky, P.D.; Guillermo Calero, G.; Christopher, J.; Ackerson, C.J.; Bushnell, D.A.; Kornberg, R.D. Structure of a thiol monolayer-protected gold nanoparticle at 1.1 Å resolution. *Science* **2007**, *318*, 430-433.
63. Mednikov E.G.; Dahl, L.F. Crystallographically proven nanometer-sized gold thiolate cluster $Au_{102}(SR)_{44}$: Its unexpected molecular anatomy and resulting stereochemical and bonding consequences. *Small* **2008**, *4*, 534-537.
64. Zhu, M.Z.; Aikens, C.M.; Hollander, F.J.; George, C.; Schatz, G.C.; Jin, R.C. Correlating the crystal structure of a thiol-protected Au_{25} cluster and optical properties. *J. Am. Chem. Soc.* **2008**, *130*, 5883-5885.
65. Qian, H.F.; Eckenhoff, W.T.; Zhu,Y.; Pintauer, T.; Jin, R.C. Total structure determination of thiolate-protected Au_{38} nanoparticles. *J. Am. Chem. Soc.* **2010**, *132*, 8280-8281.
66. Zhu, M.Z.; Aikens, C.M.; Hendrich, M.P.; Gupta, R.; Qian, H.F.; Schatz, G.C.; Jin, R.C. Reversible switching of magnetism in thiolate-protected Au_{25} superatoms. *J. Am. Chem. Soc.* **2009**, *131*, 2490-2492.
67. Zhu, M.Z.; Eckenhoff, W.T.; Pintauer, T.; Jin, R.C. Conversion of anionic $[Au_{25}(SCH_2CH_2Ph)_{18}]^-$ cluster to charge neutral cluster *via* air oxidation. *J. Phys. Chem. C* **2008**, *112*, 14221-14224.
68. Qian, H.F.; Zhu, Y.; Jin, R.C. Size-focusing synthesis, optical and electrochemical properties of monodisperse $Au_{38}(SC_2H_4Ph)_{24}$ nanoclusters. *ACS Nano* **2009**, *3*, 3795-3803.
69. Jin, R.C.; Zhu, Y.; Qian, H.F. Quantum-size gold nanoclusters: Bridging the gap between organometallic and nanocrystals. *Chem. Eur. J.* **2011**, *17*, 6584-6593.
70. Lopez-Acevedo, O.; Kacprzak, K.A.; Akola, J.; Hakkinen, H. Quantum size effects in ambient CO oxidation catalysed bu ligand-protected gold clusters. *Nat. Chem.* **2010**, *2*, 329-334.
71. Yoon, B. Charging effects on bonding and catalyzed oxidation of CO on Au8 clusters on MgO. *Science* **2005**, *307*, 403-407.
72. Kacprzak, K.A.; Akola, J.; Hakkinen, H. First-principes simulations of hydrogen peroxide formation catalyzed by small neutral gold clusters. *Phys. Chem. Chem. Phys.* **2009**, *11*, 6359-6364.
73. Prestianni, A.; Martorana, A.; Ciofini, H.; Labat, F.; Adamo, C. CO oxidation on cationic gold clusters: A theoretical study. *J. Phys. Chem. C* **2008**, *112*, 18061-18066.
74. Remediakis, I.N.; Lopez, N.; Norskov, J.K. CO oxidation on rutile-supported Au nanoparticles. *Angew. Chem. Int. Ed.* **2005**, *44*, 1824-1826.
75. Roldan, A.; Gonzalez, S.; Ricart, J.M.; Illas, F. Critical size for O_2 dissociation by Au nanoparticles. *Chemphyschem* **2009**, *10*, 248-351.
76. Corma, A.; Boronat, M.; Gonzalez, S.; Illas, F. On the activation of molecular hydrogen by gold: A theoretical approximation to the nature of potential active sites. *Chem. Commun.* **2007**, 3371-3373.
77. Turner, M.; Golovko, V.B.; Vaughan, O.P.H.; Abdulkin, P.; Murcia, A.B.; Tikhov, M.S.; Johnson B.F.G.; Lambert, R.M. Selective oxidation with dioxygen by gold nanoparticle catalysts derived from 55-atom clusters. *Nature* **2008**, *454*, 981-983.
78. Tsunoyama, H.; Ichikuni, N.; Sakurai, H.; Tsukuda, T. Effect of electronic structures of Au clusters stabilized by poly(*N*-vinyl-2-pyrrolidone) on aerobic oxidation catalysis. *J. Am. Chem. Soc.* **2009**, *131*, 7086-7093.

79. Liu, Y.; Tsunoyama, H.; Akita, T.; Xie, S.; Tsukuda, T. Aerobic oxidation of cyclohexane catalyzed by size-controlled Au clusters on hydroxyapatite: Size effect in the sub-2 nm regime. *ACS Catal.* **2011**, *1*, 2-6.
80. Tsunoyama, H.; Sakurai, H.; Negishi, Y.; Tsukuda, T. Size-specific catalytic activity of polymer-stabilized gold nanoclusters for aerobic alcohol oxidation in water. *J. Am. Chem. Soc.* **2005**, *127*, 9374-9375.